Structural and mechanical properties of hydroxyapatite coatings formed by ion-beam assisted deposition

IOP Conf. Series: Journal of Physics: Conf. Series **992** (2018) 012035 doi:10.1088/1742-6596/992/1/012035

Structural and mechanical properties of hydroxyapatite coatings formed by ion-beam assisted deposition

A Zykova[1,2,6], V Safonov[1,2], S Dudin[2], S Yakovin[2], N Donkov[3], M H Ghaemi[4], M Szkodo[4], M Antoszkiewicz[4], M Szyfelbain[5] and A Czaban[5]

[1]National Science Center "Kharkov Institute of Physics and Technology",
1 Academicheskaya Str., 61108 Kharkov, Ukraine
[2]Department of Physical Technologies, Kharkov National University,
4 Svobody Sq., 61077 Kharkov, Ukraine
[3]Emil Djakov Institute of Electronics, Bulgarian Academy of Sciences,
72 Tzarigradsko Chaussee, 1784 Sofia, Bulgaria
[4]Gdansk University of Technology, 11/12 G. Narutowicza, 80233 Gdansk, Poland
[5]Gdynia Maritime University, 81/87 Morska, 81225 Gdynia, Poland

E-mail: zykova.anya@gmail.com

Abstract. The ion-beam assisted deposition (IBAD) is an advanced method capable of producing crystalline coatings at low temperatures. We determined the characteristics of hydroxyapatite $Ca_{10}(PO_4)_6(OH)_2$ target and coatings formed by IBAD using X-ray photoemission spectroscopy (XPS), X-ray diffraction (XRD), scanning electron microscopy (SEM), atomic force microscopy (AFM) and energy dispersive X-ray (EDX). The composition of the coatings' cross-section and surface was close to those of the target. The XPS spectra showed that the binding energy values of Ca (2p1/2, 2p3/2), P (2p3/2), and O 1s levels are related to the hydroxyapatite phase. The coatings demonstrate an optimal H/E ratio, and a good resistance to scratch tests.

1. Introduction

The bioactive properties of hydroxyapatite $Ca_{10}(PO_4)_6(OH)_2$ (HAP) materials (powders, ceramics, coatings) are widely applied in the clinical practice. The osteoconductive properties of HAP-coated scaffolds have a great potential for further tissue-engineering use due to the possibilities of bone tissue reconstruction [1-3]. A pressing challenge in biomedical technology is to produce medical implants with highly bioactive and antibacterial surfaces. Modern implants made of hydroxyapatite materials, namely, HAP-coated metal prostheses, bond readily to bone without rejection or inflammatory reactions [4]. Crystalline HAP coatings with homogeneous composition are preferable because of their reduced *in vivo* dissolution [5, 6]. However, the insufficient purity and uniformity of the HAP coatings, the low crystallinity of the films and their poor adhesion to the substrate materials limit the lifetime of implants with HAP coatings. Among the techniques used for HAP coatings deposition, the ion-beam assisted deposition (IBAD) stands out as an advanced method capable of producing crystalline coatings at low-temperature, while avoiding the need of high-temperature annealing for

[6] To whom any correspondence should be addressed.

further crystallization [7, 8]. The relation between HAP coatings growth mechanisms and their properties related to biomedical applications is of great interest. Moreover, the deposition conditions affect significantly the structure, composition, biomechanical properties, and HAP coatings' capacity to promote bone regeneration.

2. Materials and methods

The aim of the present work was to study the deposition conditions effects on the structure and properties of hydroxyapatite $Ca_{10}(PO_4)_6(OH)_2$ ceramic coatings. Glass and silicon samples were used as substrates. The coatings were deposited using ion-beam sputtering of a hydroxyapatite target. The ion beam was generated by a Hall-type ion source with anode voltage of 3 kV. An oxygen ion-beam with a current density of 3 mA/cm^2 bombarded the hydroxyapatite target in the vacuum chamber. The main details of the deposition technique and conditions were presented in [7].

The deposited coatings' thickness was estimated by Calotest measurements. The surface roughness was evaluated using a Hommel Werke T8000 Profilograph. The coatings' surface structure and morphology were observed by a confocal laser microscope (LEXT OLS 4100), a scanning electron microscope (Zeiss EVO MA15 SEM) and an atomic force microscope (NT-206 AFM).

X-ray photoemission spectroscopy (XPS) was carried out using an ESCALAB MkII (VG Scientific) electron spectrometer at a base pressure in the analysis chamber of 5×10^{-8} Pa (1×10^{-6} Pa during the measurements), using an AlKα X-ray source (excitation energy hν = 1486.6 eV). The pass energy of the hemispherical analyzer is 20 eV. The instrumental resolution measured as the full width at a half maximum (FWHM) of the $Ag3d_{5/2}$ photoelectron peak is 1 eV. The energy scale is corrected to the C1s-peak maximum at 285.0 eV for electrostatic charging. The processing of the measured spectra includes a subtraction of X-ray satellites and Shirley-type background [9]. The peak positions and areas are evaluated by symmetrical Gaussian-Lorentzian curve fitting. The relative concentrations of the different chemical species are determined based on normalization of the peak areas to their photoionization cross-sections, calculated by Scofield [10].

The chemical composition of the coatings was analyzed by energy dispersive X-ray (EDX) spectroscopy (X Flash 6/30, Bruker). The adhesion properties were evaluated using standard methods by a Revetest device (CSM Instrumets). The nano-indentation tests were performed using a nano-indenter fitted with a three-sided pyramid Berkovich indenter. The loading and unloading sequences were standard [11]. Repeated indentations were performed, and the values were calculated as the average of 10 indentations.

3. Results and discussion

The target phase composition was analyzed by XRD in the range θ-2θ by a DRON-3 device in FeKα radiation (table 1). The diffraction pattern is presented in figure 1.

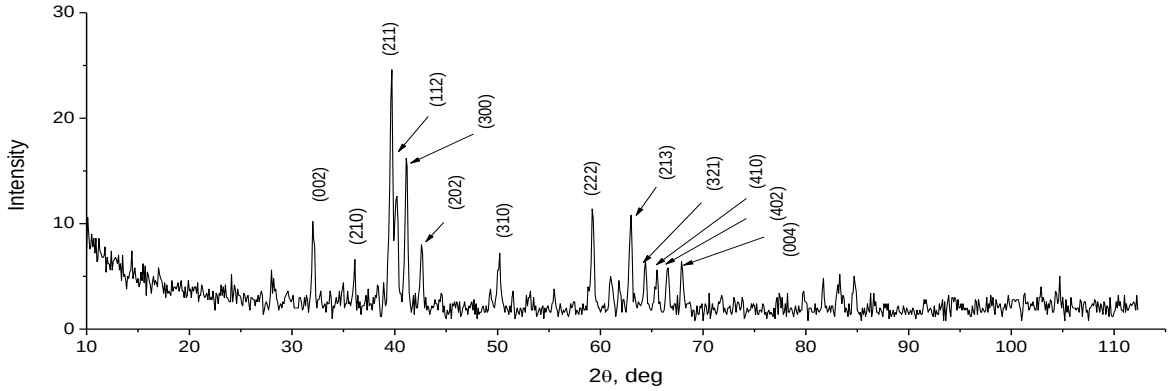

Figure 1. Diffraction peaks of the $Ca_{10}(PO_4)_6OH_2$ target composition.

The diffraction lines correspond to hydroxyapatite $Ca_{10}(PO_4)_6OH_2$ of hexagonal syngony. The main peaks are marked. The lattice parameters of the HAP target were evaluated from the position of (300) and (004) lines and were about $a = 0.955 \pm 0.001$ µm and $c = 0.693 \pm 0.001$ µm. In the case of evaluation from the (410) line, the lattice parameter was about $a = 0.924 \pm 0.001$ µm (table 1). No peaks of other compounds were detected.

Table 1. Crystal lattice parameters of the $Ca_{10}(PO_4)_6OH_2$ target.

(hkl)	2θ.deg	d, µm	a, µm	c, µm
(300)	41.10	0.27595	9.55	
(410)	65.50	0.17905	9.24	
(004)	67.97	0.17326		6.93

XRD diffractograms of coatings deposited on glass substrate were presented earlier [12]. The main peaks attributed to the HAP crystalline structure (JPCDS 9-0432) were observed, indicating that a crystalline HAP phase was obtained. This is an important result, because it has been demonstrated that amorphous or less crystalline phases are more soluble in contact with body fluids, leading to a high dissolution rate, which affects the long-term stability of an implant [13-15].

In view of characterizing in further detail the HAP coatings' elemental and stoichiometric composition, we conducted EDX and XPS analyses.

The EDX results revealed the same peaks of Ca, P in the target and in the coating's cross-section and surface (figure 2). The target composition was stoichiometric, with a Ca/P ratio of about 1.67.

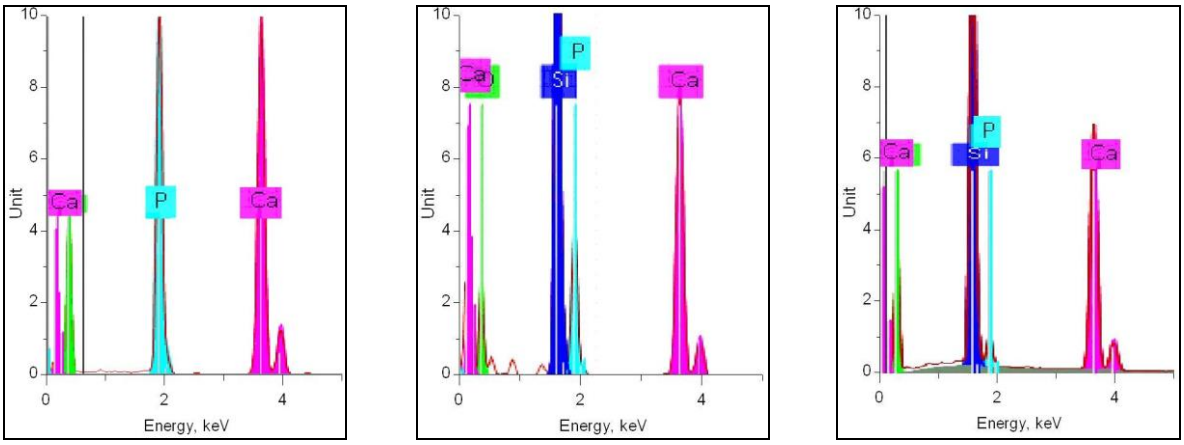

a) b) c)

Figure 2. EDX spectra of $Ca_5(PO_4)_3(OH)$: a) target, b) cross-section, c) surface of coatings deposited on Si substrate.

The composition of the coating's cross-section and surface was close to that of the target. The main elements (Ca, P) were uniformly distributed in both the cross-section and surface of coating, indicating the formation of a homogenous structure. The XPS spectra of O 1s, Ca 2p, and P 2p core levels were recorded in view of analyzing the chemical bonding (figure 3).

The binding energy of O 1s attributed to the PO_4 bond of hydroxyapatite was 531.6 eV. The binding energy of Ca 2p3/2 was 347.8 eV and that of Ca 2p1/2 was 350.7 eV, all related to hydroxyapatite. The P 2p spectrum presented a peak for the p3/2 level with a binding energy of 133.6 eV, which corresponds to P in the hydroxyapatite. The binding energy values of Ca 2p, P 2p, and O1s levels are strongly related to the hydroxyapatite phase [16]. The surface atomic concentration is presented in table 2.

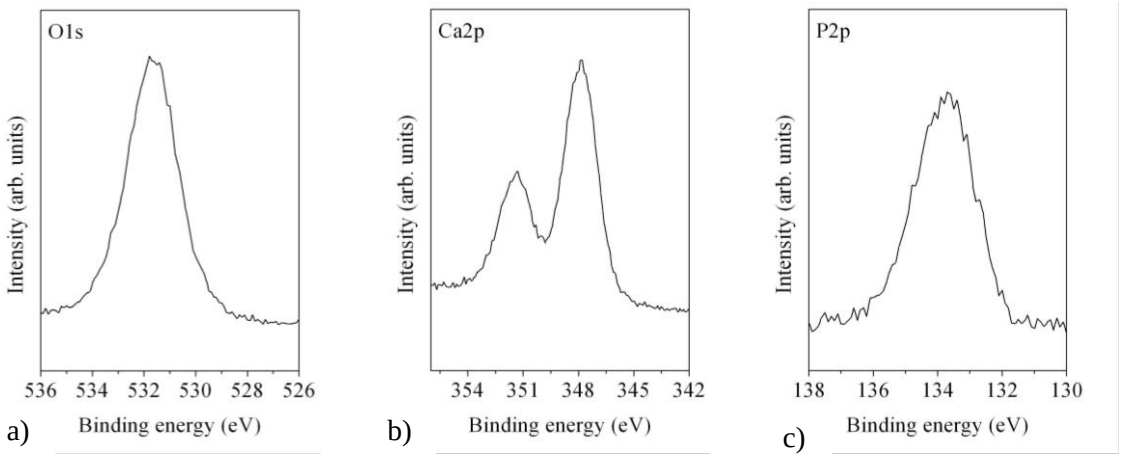

Figure 3. XPS spectra: a) O 1s, b) Ca 2p, c) P 2p core levels.

The surface topography and morphology of the coatings of $Ca_{10}(PO_4)_6(OH)_2$ were observed by SEM and AFM (figure 4). The main parameters of the coatings – thickness, adhesion strength, and surface roughness are presented in table 3.

The nano-indentation tests were conducted at different loads using a constant loading rate. The loading–unloading curves were used to determine the hardness H and the elastic modulus E (table 4).

Table 2. Surface atomic concentration.

Sample\Elements	O 1s, at. %	Ca 2p, at. %	P 2p, at. %
$Ca_{10}(PO_4)_6OH_2$	53	29	18

Table 3. Coating thickness, adhesion strength and surface roughness.

Coating	Thickness, μm	Adhesion strength, N	Roughness Ra, μm	Roughness Rz, μm
$Ca_{10}(PO_4)_6OH_2$	1.8	9.31	0.077	0.602

Table 4. Coating hardness H, elastic modulus E, and plastic resistance ratio parameters.

Coating	H, GPa	E, GPa	H/E	H^3/E^2, GPa
$Ca_{10}(PO_4)_6OH_2$	6.21±0.97	108.6±4.1	0.057	0.021

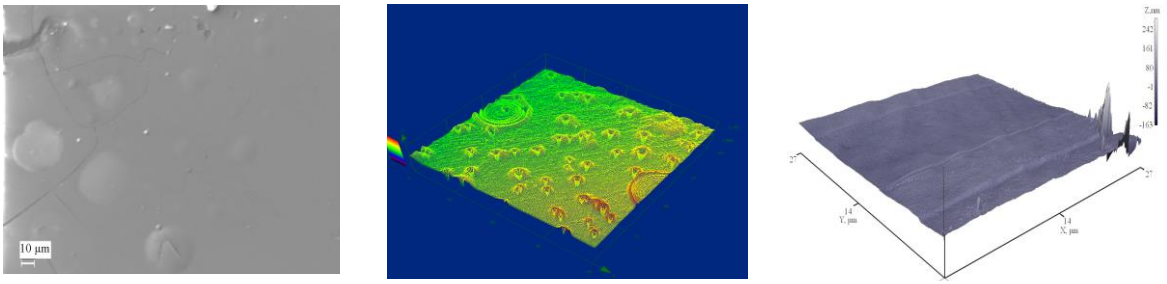

a) b) c)

Figure 4. Surface roughness and morphology of $Ca_{10}(PO_4)_6(OH)_2$ coatings: a) SEM image of a coating surface, b) 3D confocal laser microscope image of the coating's surface, c) 3D AFM image of the coating's surface.

HAP has a higher elastic modulus than natural bone. The difference in this parameter between bone and coating results in greater stress concentration and fractures at the bone-implant interfaces [17].

The H/E ratio can be attributed to a good wear resistance of the material and demonstrates the elastic strain to failure [18]. Materials with a high plastic resistance ratio H^3/E^2 have exhibited a higher yield strength [19]. An optimal H/E ratio results in increased durability of the surface of biomaterials.

The adhesion of the CaP coating to the surface of implants and scaffolds is a very important parameter, which affects the performance and longevity of the medical devices. Adhesion failures result in delamination of the coating and loosening of the implant, thus leading to mechanical failure and bone resorption. Various treatment procedures have been realized to improve the adhesion strength of hydroxyapatite coatings on substrates. Scratch test results have shown that the adhesion strength of the HAP coating on substrates was in the range 2.60 N – 3.14 N depending on the treatment conditions [20]. The effect of an oxide interlayer on the adhesion strength of HAP coating on oxidized Co-Cr-Mo substrate was investigated in [21]. The results demonstrated that the formation of interlayers improves the adhesion strength between coatings and metals in the range 1.40 N – 1.04 N. In the present study, we found an adhesion strength of hydroxyapatite coatings to the substrates of about 9.31 N, a value higher than those reported earlier.

The results presented in the study confirmed that IBAD is a highly reliable, reproducible technique for creating thin, defect-free HAP coatings. The method allows accurate control of the HAP growth parameters at low deposition temperatures with capability of producing highly crystalline coatings [22]. The sputter cleaning process removes contaminants and gas molecules adsorbed on the surface of the substrate to produce a clean, highly-active surface. Furthermore, the process allows superior control over the coatings' microstructure and chemical composition [23].

4. Conclusions

The results demonstrate the strong effect of the sputtering process conditions on the coating structural and surface properties. IBAD using allows one to produce high-quality coatings due to the high-energy ion bombardment process. The general conclusions about the quality of hydroxyapatite $Ca_{10}(PO_4)_6(OH)_2$ coatings were drawn on the basis of the results from EDX, XPS, AFM, SEM measurements. According to the energy-dispersive X-ray analysis, the Ca/P ratio of the deposited HAP coatings reaches values similar to those of the HAP target. The adhesion strength of the hydroxyapatite coatings has values higher than those reported previously. The coatings possess an optimal H/E ratio, a good resistance to scratch tests, and improved biomechanical properties for further advanced biomedical applications.

Acknowledgments

The study was supported under the Towards Intelligent Micro-Bearing Tribological Aspects Project (ImBeing-FP7-PEOPLE-2013-IRSES-612593) and a BAS-NASU Cooperation Agreement.

References

[1] Russo A, Bianchi M, Sartori M, Boi M, Giavaresi G, Salter DM, Jelic M, Maltarello M C, Ortolani A, Sprio, Fini M, Tampieri A and Marcacci M 2017 *Biomed. Mater. Res.* B doi: 10.1002/jbm.b.33836
[2] Huang Y, Zhang X, Zhang H, Qiao H, Jia T, Han S, Gao Y, Xiao H and Yang H 2017 *Ceramics Int.* **43** 992
[3] Zykova A, Safonov V, Smolik J, Rogowska R, Donkov N, Goltsev A and Dubrava T 2012 *J. Phys.: Conf. Series* **356** 012040
[4] Liu H and Webster T J 2007 *Biomater.* **28** 354
[5] Baltag I, et al. 2000 *Biomed. Mater. Res*. **53** 76
[6] Yang Y, Kim K H and Ong J 2005 *Biomater*. **26** 327
[7] Donkov N, Zykova A, Safonov V, Kolesnikov D, Goncharov I and Yakovin S 2014 *J. Phys.: Conf. Series* **514 0**12017
[8] Ozeki K, Goto T, Aoki H and Masuzawa T 2015 *Biomed. Mater. Eng*. **26** 139
[9] Shirley D 1972 *Phys. Rev.* B **5** 4709

[10] Scofield J H 1976 *Electron Spectrosc. Relat. Phenom.* **8** 129
[11] Fischer-Cripps A C 2011 *Nanoindentation* p 280 (New York, Springer)
[12] Dudin S, Cotrut C M, Dinu M, Zykova A, Parau A C, Yakovin S and Vladescu A 2017 *Ceramics Int.* doi: 10.1016/j.ceramint.2017.08.016
[13] Zykova A, Safonov V, Yanovska A, Sukhodub L, Rogovskaya R, Smolik J and Yakovin S 2015 *Open Biomed. Eng.* **9** 75
[14] Zhang Q, Chen J, Feng J, Cao Y, Deng C and Zhang X 2003 *Biomater.* **24** 4741
[15] Xue W, Tao S, Liu X, Zheng X and Ding C 2004 *Biomater.* **25** 415
[16] Rulis P, Ouyang L and Ching WY 2004 *Phys. Rev.* B **70** 155104
[17] Roop R, Kumar R and Wang M 2002 *Mater. Sci. Eng.* A **338** 230
[18] Leyland A and Matthews A 2000 *Wear* **246** 1
[19] Musil J 2000 *Surface and Coating Technol.* **125** 322
[20] Grubova I, Priamushko T, Surmeneva M, Korneva O, Epple M, Prymak O and Surmenev R 2017 *J. Phys.: Conf. Ser.* **830** 012109
[21] MasAyu H, Izman S, Daud R, Krishnamurithy G, Shah A, Tomadi H and Salwani MS 2017 *Procedia Eng.* **184** 399
[22] Cui F and Luo Z. 1999 *Surf. Coat. Technol*. **112** 278
[23] Ozeki K, Yuhta T, Fukui Y and Aoki H. 2002 *Surf. Coat. Technol*. **160** 54